#3937

The Velocity Characteristics of Ventilated Rooms

P. V. NIELSEN

A. RESTIVO

J. H. WHITELAW

Imperial College of Science and Technology, Mechanical Engineering Department, Fluids Section, London, England

Measured and calculated values of the velocity characteristics of a modeled room with ventilation arrangements are reported. The measurements were obtained by laser-Doppler anemometry and the calculations by the solution, in finite-difference form, of two-dimensional, elliptic, partial-differential equations representing conservation of mass, momentum, turbulence energy and dissipation rate. The results demonstrate that the precision of calculation is adequate for design purposes although, for slots much smaller than the width of the room, three-dimensional effects become important. They quantify, for example, the extent to which a decrease in supply area leads to an increase in air velocities for a given mass flow rate.

1 Introduction

The velocity characteristics of ventilated rooms are important in that they help to control the comfort and well being of individuals. Temperature, radiation and humidity are also important and their influences represent an extension of the present paper which reports calculated and measured velocity values and their dependence on geometry and inlet flow arrangement. The calculated values were obtained by solving two-dimensional, elliptic, partial-differential equations and the validity of these equations is assessed by comparison with measurements, obtained by laser-Doppler anemometry, in model rooms.

Previous experimental investigations of the flow in air-conditioned rooms have been reported, for example by Linke [1], Müllejans [2], Urbach [3], Jackman [4], Schwenke [5], Hestad [6, 7] and Nielsen [8]. Those of Hestad and Jackman were carried out in full-scale rooms and the other authors made use of models which allowed the advantage of improved measurement accuracy as a consequence of the higher velocities associated with the same Reynolds number. The model experiments of Müllejans and Schwenke made use of flow visualization and, consequently, were of a qualitative nature; other investigations used probes and are subject to unknown uncertainty in regions of high turbulence intensity and flow recirculation. These previous experimental investigations were mainly intended to provide support for simple design procedures, based on correlation equations.

To avoid the need for extensive experimentation, Nielsen [9] attempted to develop a calculation procedure which would allow the prediction of the flow patterns in ventilated rooms. This work was based on the stream-function approach of Gosman, et al. [10] and is not readily extended to three-dimensional flows. In addition, comparison of calculated results with measurements indicated the need for improvement in both calculation and measurement techniques. For example, previous numerical work made use of a scheme with poor convergence performance and previous measurements used instrumentation, as indicated above, which is inappropriate to significant regions of ventilation flows.

The present calculations were obtained by solving equations with velocities as dependent variables and are, therefore, readily extended to three-dimensional flows. The method makes use of a two-equation turbulence model which, as demonstrated by Pope and Whitelaw [11] and Gosman, Khalil, and Whitelaw [12], is probably the most advanced model which can be justified on present knowledge. In addition, and to overcome numerical problems associated with a jet of small dimension issuing into a room of large dimensions, calculations have been performed with initial wall-jet development assumptions.

The experiments make use of laser-Doppler anemometry which does not interfere with the flow and is able to correctly resolve the sign as well as the magnitude of velocity. The measured velocity values are compared with corresponding calculations in order to allow the procedure, with inherent assumptions, to be appraised and quantitatively assessed over a practical relevant range of parameters. Calculated results, of significance to air conditioning and outside the range of existing measurements, are then presented and discussed.

The flow configuration used for the experimental investigation, the laser-Doppler anemometer and measurements are described in the following section. The calculation method and associated assumptions are presented in section 3. Calculated results and comparisons are reported in section 4 and discussed in the context of air conditioning requirements. Summary conclusions are presented in section 5.

Contributed by the Fluids Engineering Division for publication in the JOURNAL OF FLUIDS ENGINEERING. Manuscript received by the Fluids Engineering Division, August 16, 1977.

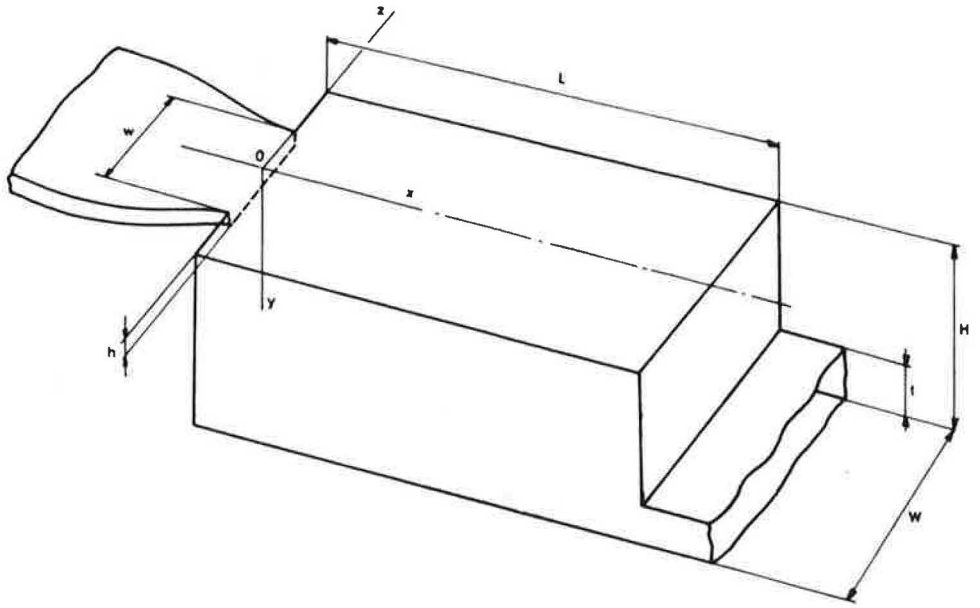

Fig. 1 Geometrical arrangements and coordinate system

2 Flow Configuration, Measurement Technique and Results

The geometrical arrangements used for the present measurements may be represented by Fig. 1 which also indicates the coordinate system used. The model was constructed from perspex with a height of 89.3 mm; other dimensions correspond to

$$L/H = 3.0; W/H = 1.0; h/H = 0.056; t/H = 0.16; w/W = 0.5 \text{ and } 1.0.$$

Two values of the width of the inlet slot were used to assist the determination of the extent of influence of a three-dimensional inlet flow on the velocity characteristics of the room. The inlet was preceded by a smooth, plane contraction of area ratio 2 and resulted in the initial profiles shown on Fig. 2. As can be seen, the mean profiles are symmetric about $y = 0.5h$ and closely correspond to developed turbulent channel flow; the corresponding profiles of rms of velocity, normalized with U_0, are near uniform with a center value corresponding to an intensity $\tilde{u}/U$ of 0.04. Spectrum analysis of the velocity signal indicated typical turbulence spectra for Reynolds numbers above around 4000. Transverse profiles along the centerline of the slot indicate, over the central 80 percent of both slots, differences of less than two percent of the bulk velocity. Measurements obtained at Reynolds numbers from 5000 to 10,000 (and not presented for reasons of space) show that, within experimental uncertainty, nondimensional profiles are independent of Reynolds number for each geometry.

The determination of mean velocities and the corresponding rms values were obtained with a laser-Doppler anemometer, used in accordance with the recommendations of Durst, Melling and Whitelaw [13]. It comprised a 5mW helium-neon laser, a diffraction grating similar to that described by Wigley [14], a lens and pinhole arrangement to collect forward scattered light from within the intersection region of the focussed +1 and −1 order beams from the grating, and a photomultiplier. The air supplied to the model room was passed through atomizers similar to those described, for example, by Melling and Whitelaw [15] and allowed near-continuous Doppler signals which were analyzed with the help of a frequency-tracking demodulator (Cambridge Consultants CC01). The grating was operated with

Nomenclature

$\underline{a}$ = boundary surrounding wall jet
$\underline{b}$ = boundary surrounding wall jet
C_1, C_2 = constants in modeled ϵ-equation
C_D = constant in dissipation term of K-equation
C_μ = constant in expression for effective viscosity
$C_U, C_{\delta U}, e_U, \delta_U$ = constants in correlation equations for wall jet
G = generation of turbulence energy
h = inlet slot height in room or model
H = height of room or model
K = turbulence energy
L = length of room or model
P = pressure
Re = Reynolds number ($=\rho U_0 h/\mu$)
S_ϕ = source term in general conservation equation
t = outlet slot height in room or model
U, V = components of mean velocity
$\tilde{u}, \tilde{v}$ = components of fluctuating velocity
U_0, V_0 = components of inlet velocity
U_m = maximum velocity across jet
U_{rm} = maximum velocity in reverse flow
w = width of inlet slot
W = width of room or model
x, y, z = coordinates
x_a, y_b = coordinates of wall jet boundaries
x_p = distance measured along periphery of room or model
α = angle of inlet velocity
σ_K = constant in modeled K-equation
σ_ϵ = constant in modeled ϵ-equation
Γ_ϕ = exchange coefficient in general conservation equation
ϕ = variable in general conservation equation
μ = laminar viscosity
μ_t = turbulent viscosity
μ_{eff} = effective viscosity
ϵ = dissipation rate of turbulence energy
ρ = fluid density

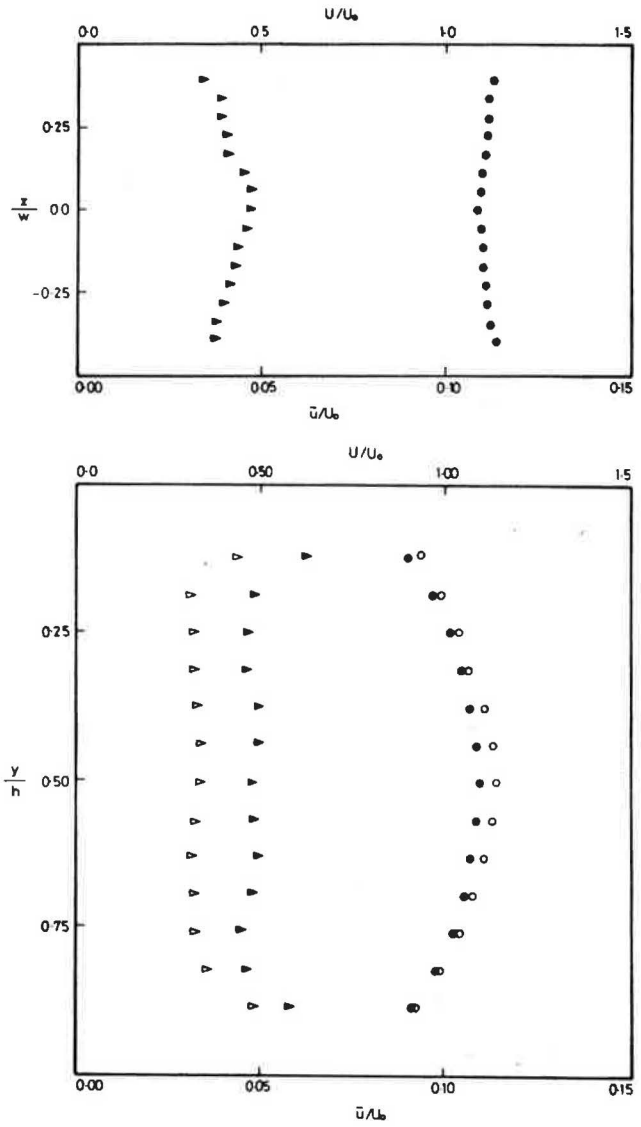

Fig. 2 Measured inlet velocity profiles. $w/W = 1.0$, **Re = 5,000**

(a) $y = h/2$. • U/U_0; ▶ $\bar{u}/U_0$

(b) z/w	U/U_0	$\bar{u}/U_0$
0.0	•	▶
−0.4	O	▷

rotational velocities and direction which allowed the frequency-tracking demodulator to be used to best advantage. The effective diameter of the measuring volume was 180 μm and a fringe spacing of 4.3 μm insured that transit time and gradient broadening effects were small and readily approximated. The largest source of error results from the instability of the rotating grating, particularly at low rotational speeds. It is estimated that the precision of measurements of mean velocity is better than 0.5 percent for velocities above 0.5 m/s. At this velocity, which corresponds to a value of U/U_0 of 0.033 on the present figures, the disk was rotated at 1000 rpm. The corresponding uncertainty in the value of $\bar{u}/U$ was less than 0.01. In both cases, the error tended to be random and is consistent with the scatter, about smooth curves, suggested by Figs. 2 and 3. The uncertainties increased, as a percentage of the local values, with diminishing U/U_0 and $\bar{u}/U$ but do not have a significant influence on the present discussion or conclusions. Systematic errors, due to the various broadening effects, were negligible compared to the random variation in disk speed for velocities less than 0.5 m/s and are considered in the 0.5 percent precision quoted for higher velocities.

Fig. 3 presents profiles of the longitudinal velocity component at two values of z and for two inlet arrangements; additional measurements confirm that the flows were symmetric about the mid-plane within measurement precision. As can be seen, the full-width entrance slot results in profiles at x/L of 2/3 which suggest that, in the region $-0.4 < z/w < 0.4$, the flow is close to two-dimensional. For the shorter slot, corresponding profiles show clearly that the flow is three-dimensional even in this central region of the model. Both sets of measurements indicate a major region of recirculation; additional measurements, again not presented for reasons of space, indicated two smaller regions of recirculation in the bottom left-hand corner and top right-hand corner of the model.

In addition to the mean velocity results of Fig. 3, corresponding values of the normalized rms velocity were obtained. They are not presented in graphical form since, when normalized with the bulk inlet velocity, (i.e. $\bar{u}/U_0$) they were less than 0.15 and, except in the vicinity of the inflections in the mean velocity distributions, very close to uniform. In the vicinity of the mean velocity inflections at larger values of x/H, the rms measurement increased to values of $\bar{u}/U_0$ of around 0.2.

The mean velocity profiles of Fig. 3 confirm the wall-jet behavior of the flow downstream of the entrance slot. They show, for example, that with the present initial conditions, the growth rate is similar to that obtained in an idealized wall-jet configuration by Schwarz and Cosart [16]. Fig. 4 presents measurements of the maximum velocity decay obtained in the wall-jet configurations of Fig. 3. These more detailed measurements, which include the half-width slot geometry, are compared with the corresponding results of Schwartz and Cosart. It is clear from this figure that both geometries lead to a wall-jet configuration, although the details of the flow and in particular the peak velocities are significantly dependent upon the initial geometry.

3 Calculation Procedure

The calculation procedure made use of the TEACH computer program devised by Gosman and Pun [17] and used extensively by many authors. It solves equations of the type

$$\frac{\partial}{\partial x}(\rho U\phi) + \frac{\partial}{\partial y}(\rho V\phi) = \frac{\partial}{\partial x}\left(\Gamma_\phi \frac{\partial \phi}{\partial x}\right) + \frac{\partial}{\partial y}\left(\Gamma_\phi \frac{\partial \phi}{\partial y}\right) + S_\phi$$

by expressing them in finite-difference form and making use of line by line iteration, and includes a pressure-correction approach to obtain solutions which satisfy mass conservation. In the present calculations, the dependent variable, ϕ, corresponds to two components of mean velocity, U and V, and to the turbulence kinetic energy κ and to dissipation rate ϵ. This two-equation turbulence model was used in the form described by Pope and Whitelaw [11]. In the vicinity of walls, the finite-difference mesh was linked to the walls by means of the wall functions described in reference [11]. The values of Γ_ϕ and S_ϕ correspond to the dependent variables and the associated properties are listed in Appendix 1.

A particular difficulty associated with the use of finite-difference methods to represent the flow in a large room supplied by a small slot lies in the distribution of grid nodes and particularly in the correct representation of the slot flow. This difficulty is compounded by the different arrangements used in previous experiments (see Fig. 5) and by the influence of the shape of the U- and V- velocity profiles in the slot exit. It is well known from the extensive wall-jet literature that the

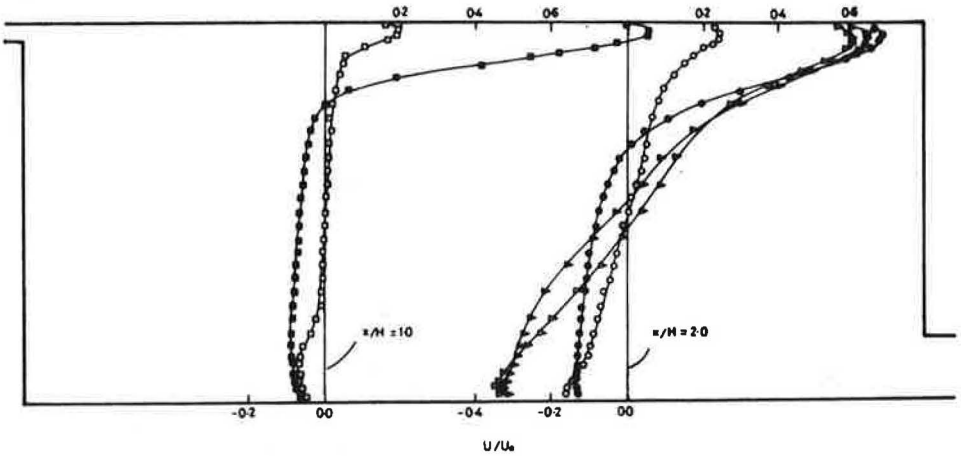

Fig. 3 Measured mean velocity profiles. Re = 5,000

w/W	x/H	z/W = 0.0	z/W = −0.4
1.0	2.0	▶	▷
0.5	1.0	■	□
0.5	2.0	●	○

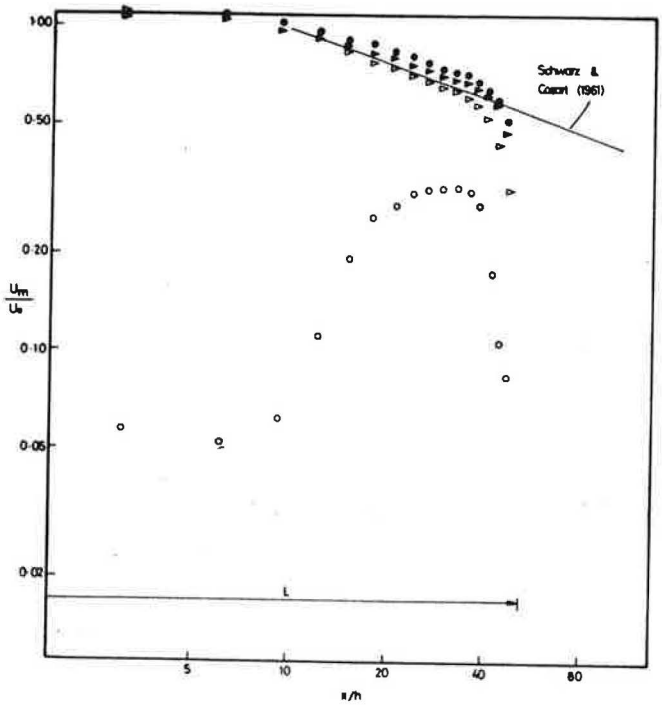

Fig. 4 Measured profiles of peak velocity in jet, Re = 5,000

w/W	z/W = 0.0	z/W = −0.4
1.0	▶	▷
0.5	•	O

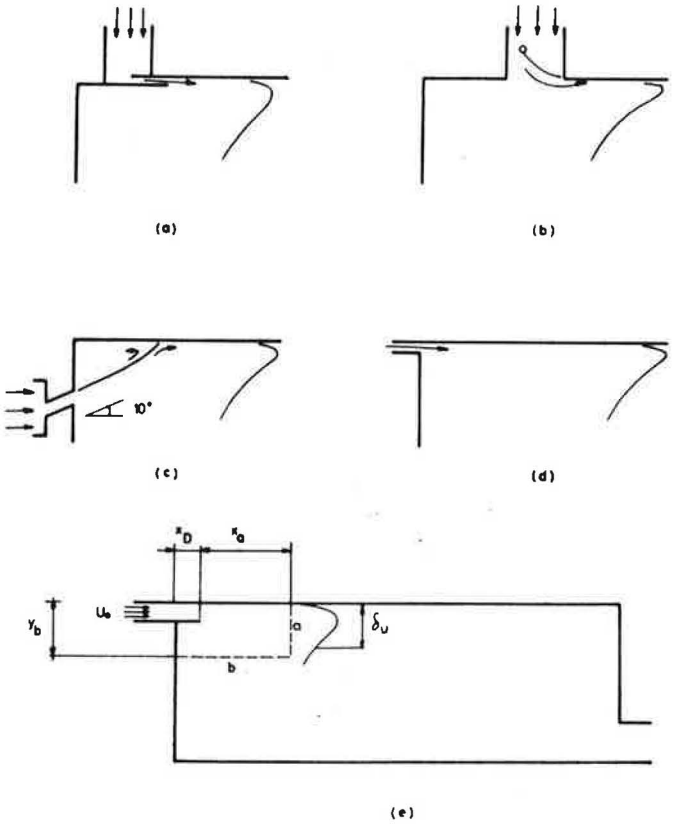

Fig. 5 Different arrangements. (*a*) Hostad (1971); (*b*) Linear diffuser; (*c*) Hostad (1974); (*d*) present measurements; (*e*) parameters used in wall jet assumptions.

decay in maximum velocity and associated spreading rate are influenced by initial conditions and yet it is not economically practical to represent the slot flow by a large number of grid nodes for more than sample calculations. As a consequence, present calculations were obtained with boundary conditions assigned along the solution domain indicated on Fig. 5(*e*). Line *a* is assumed to be in the fully developed region of the jet and its precise location is unimportant provided that x_a is kept small compared to the length of the room. The location of line *b* and the values of variables along it have little influence on the calculated results, because this boundary acts as an outlet for the remaining flow field.

For the comparisons indicated on Fig. 7, experimental velocity profiles were used along *a*; the *K*-distribution was taken from the measurements of Nelson [18] and the ϵ-distribution was determined assuming a simple linear variation of the length scale up to a constant level across the jet. Along line *b*, as well

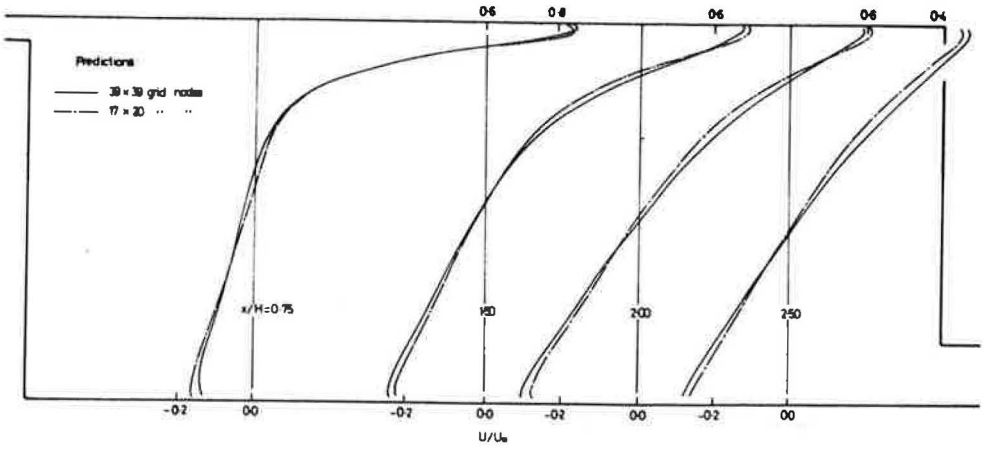

Fig. 6 Comparison between predictions obtained with different numbers of grid nodes

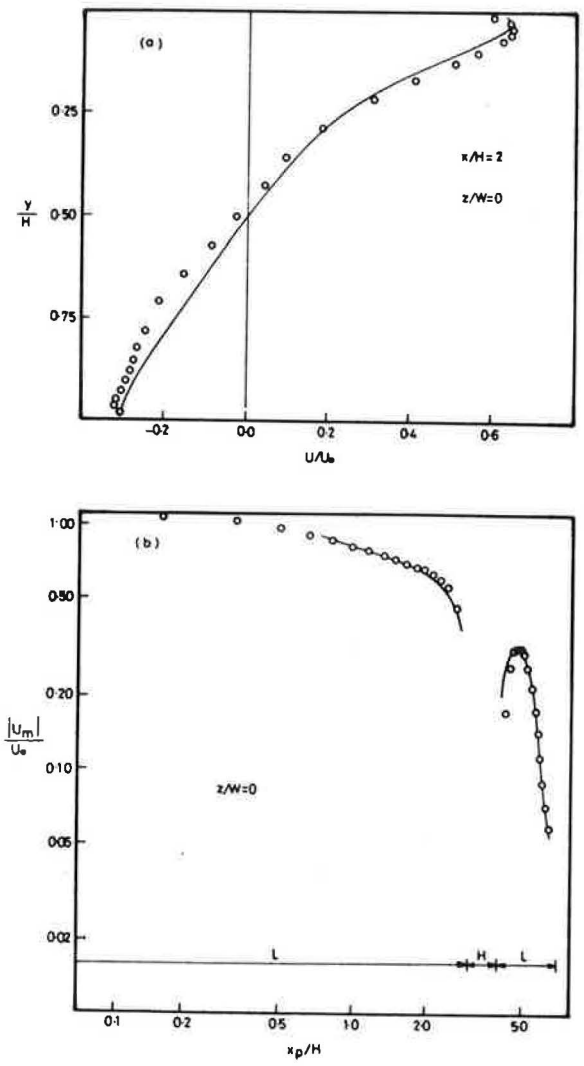

Fig. 7(a, b) Present measurements

as at the exit, zero streamwise gradients were imposed to all variables. For other details see Nielsen [8]. In the air-conditioning industry (see for example ASHRAE Handbook of Fundamentals [19]), profiles of the form used along a have been characterized by correlation equations which are indicated together with coefficients in Appendix 2.

4 Calculated Results and Discussion

The influence of the number of grid nodes was tested and a sample of the results is shown in Fig. 6. These calculations correspond to the present flow configuration and it is clear that, although 17 × 20 grid nodes led to a "converged" solution, 39 × 39 grid nodes led to a different "converged" solution. The two sets of results are very similar but careful inspection shows discrepancies of up to three percent. This magnitude of uncertainty is likely to remain with all practically possible numbers of grid nodes.

Four sets of experimental data, obtained with different geometric arrangements, are used to appraise the capabilities of the present procedure. Their characteristics are indicated below:

Table 1

Data	L/H	h/H	W/H	w/W	Re
Present investigations	3.0	0.056	1	1.0	5,000
Nielsen (1976)	3.1	0.056	4.7	1.0	7,100
Hestad (1971)	3.0	0.005	1.2	1.0	1,800
Hestad (1974)	1.9	0.003	0.9	1.0	1,400

All calculations were performed with approximately 20×20 grid nodes and required around 100 s of computing time on a CDC 6600.

The comparisons shown in Figs. 7(a) and (b) relate to the present measurements obtained along the centerline of the model with the full-width opening. It is clear that the general features of the measurements are correctly represented by the calculations, although some discrepancies occur, particularly in the area of reverse flow. This was expected, since three-dimensional effects are present, as can be seen in Fig. 3. Fig. 7(b) compares peak U-velocities across the jet, plotted against the distance from the inlet measured along the perimeter of one longitudinal section (x_p).

Fig. 7(c) compares the present calculations with measurements obtained in a model with larger W/H ratio, i.e. that of Nielsen [8]. The measured values were obtained with hot wire anemometry but are confined to regions of the flow where interference and signal interpretation errors are unlikely to be important. In the calculations, initial conditions were prescribed according to Schwarz and Cosart [16]. The agreement is excellent except in the incoming jet. This might have been improved if the correct inlet profiles were known from experiments.

The results of Hestad [6, 7] were obtained with smaller h/H ratio, in full-scale rooms. Fig. 7(d) shows the fast decay

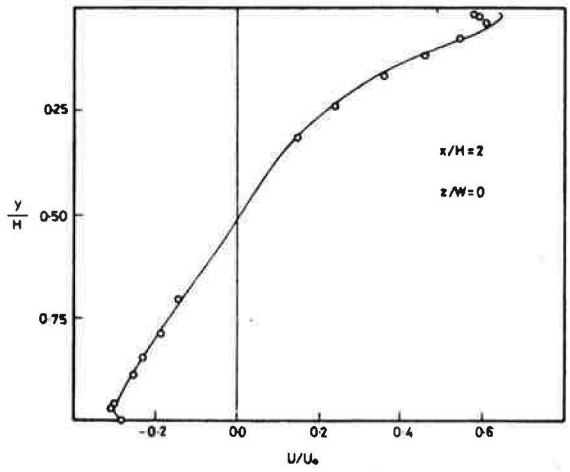

Fig. 7(c) Nielsen (1976)

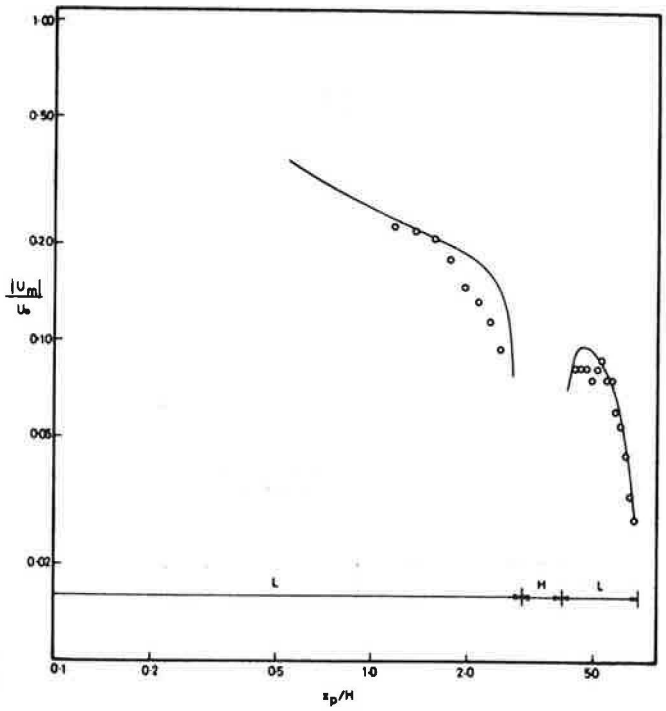

Fig. 7(d) Hestad (1971)

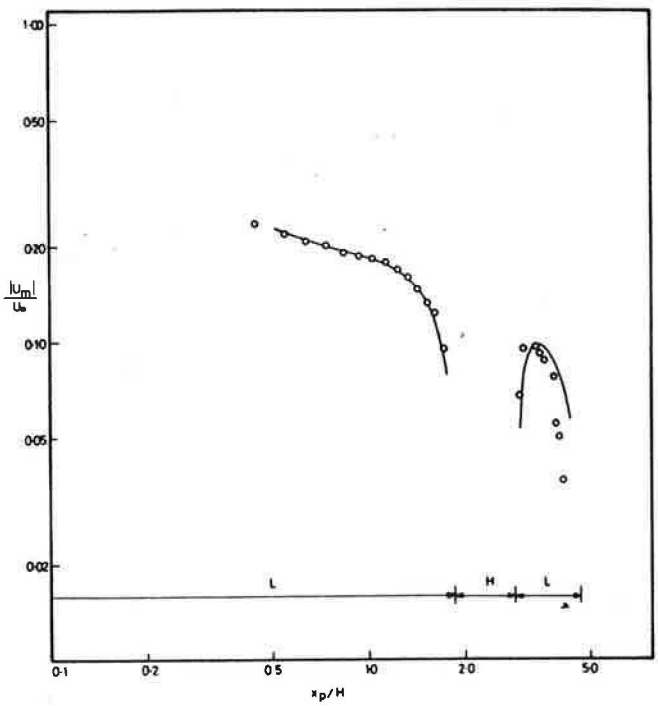

Fig. 7(e) Hestad (1974)

Fig. 7 Comparisons between predictions and experiments

of the jet peak velocity, which is likely to have been accelerated by light fittings in the test room. Apart from this discrepancy, the agreement is good. Fig. 7(*e*) presents a similar comparison for a room with a different inlet arrangement, consisting of a slot displaced from the ceiling, as in Fig. 5(*c*). The agreement is of the same order as in Nielsen's experiments. For both sets of measurements, predictions made use of measured data for the initial jets.

In general, the comparisons of the previous paragraphs confirm that the calculation procedure is able to represent the trends observed experimentally and, except perhaps in regions of low velocity, to represent the measured velocities within ±5 percent. Care has been taken to prescribe measured inlet conditions whenever they were available. In air-conditioning practice several types of diffusers are used, and result in different inlet profiles of both U- and V-velocities, and sometimes separation of the jet from the ceiling and subsequent reattachment. Important differences between the flow patterns produced by such diffusers may be expected.

The present calculation procedure was used to assess the influence of an initial V-component, V_0, on the maximum velocity in the return flow. Calculations were performed over the entire flow field and relate to a large value of h/H, as imposed by grid size limitations. Results are contained in Fig. 8 which also shows U-velocity profiles across the initial jets for several inlet angles. Clearly, the maximum reverse velocity U_{rm} is reduced as the inlet angle increases, and the effect is strong: a deflection of 20 deg alters the velocity by ten percent.

Calculated values of the maximum reverse-flow velocity are presented in Fig. 9 as a function of the inlet opening and for three values of room length; the initial profiles were specified according to the data of Schwarz and Cosart [16]. Information of this type is particularly relevant to air-conditioning design since it provides a rapid overview of the maximum velocities likely to be experienced by room occupants. It is clear that the maximum reverse-flow velocity increases with increasing supply opening and decreasing room length for constant inlet velocity. Fig. 9 also presents results obtained with initial profiles from Schwartzbach [20] and appropriate to an inlet opening displaced 0.075H from the ceiling; comparison of the velocity profiles of Figs. 8 and 9 indicates that a jet with a positive V-velocity and a reattaching jet both give rise to wall jets with virtual origins further upstream of the inlet plane and, consequently, to lower peak velocities.

Closer examination of Fig. 9 shows that, for narrow slots, the maximum reverse velocity normalized by the bulk inlet velocity, tends to vary as $(h/H)^{0.5}$. In practice, where the flow rate is partly dependent upon air refreshment requirements, this implies that a reduction of h is accompanied by an increase of U_{rm}, i.e. $U_{rm} \sim h^{-0.5}$ approximately. The dependence of U_{rm} on the length of the room is also clear; longer rooms give rise to lower velocities, for the same inlet geometry.

Longer rooms may also give rise to unsteady flows, as observed by Nielsen [8] for L/H ratios of 4.5 and over.

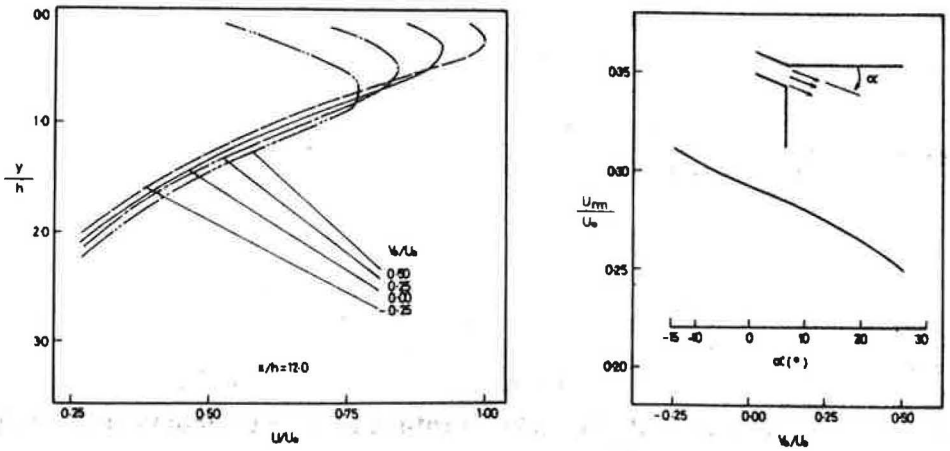

Fig. 8 Influence of angle of diffuser on maximum velocity in reverse flow prediction. h/H = 0.056; L/H = 3.0.

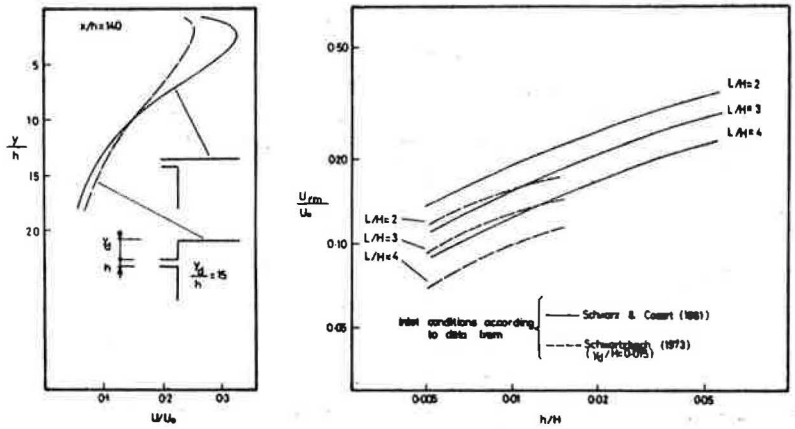

Fig. 9 Influence of room length and slot height on maximum velocity in reverse flow (prediction)

5 Conclusions

The following paragraphs provide a summary of the more important conclusions which may be extracted from the present work.

1. It is possible, by solving appropriate elliptic-differential equations in finite-difference form, to represent the velocity characteristics throughout a ventilated room. The precision of the results, as demonstrated by comparison with measurements, is adequate for design purposes.
2. Since the supply openings are usually of small dimensions, detailed information of the jet flow as a function of inlet geometry is required at a downstream location where the width of the wall-jet is greater than that of the supply opening. Further research is required to allow general calculations but, for a practically important range of geometries, this information is available and useful design calculations can be performed.
3. It has been shown that the flow in air conditioned rooms can be represented by two-dimensional equations over much of the width provided the supply opening is not much shorter than the width of the room.
4. The results quantify the extent to which, with a given air flow rate, a decrease in supply area leads to an increase in the air velocities in the room.
5. Further work is necessary to characterize the flow throughout rooms with small supply openings and long rooms where flow instabilities may be expected.

Acknowledgments

The authors wish to acknowledge personal financial support from the Danish Government Fund for Scientific and Industrial Research (PVN) and from Comissão Permanente INVOTAN and Instituto Nacional de Investigacão Cientifica (AR). Danfoss A/S (PVN) and the University of Oporto (AR) kindly released their staff to allow this work to be carried out. The experimental and computational work was supported by the Science Research Council to whom all authors record their thanks.

Dr. A. D. Gosman contributed to this work through several valuable technical discussions; in addition, the computer program owes much to his efforts and we are especially glad to have the opportunity to acknowledge his contributions.

References

1 Linke, W., "Strömungsvorgänge in zwangsbelüfteten Räumen," VDI-Berichte Bd. 21, 1957.
2 Müllejans, H., "Über die Ähnlichkeit der nicht-isothermen Strömung und den Warmeübergang in Räumen mit Strahllüftung," Diss. T. H. Aachen, 1963.
3 Urbach, D., "Modelluntersuchungen zur Strahllüftung," Diss. T. H. Aachen, 1971.
4 Jackman, P. J., "Air Movement in Rooms With Ceiling-Mounted Diffusers," The Heating and Ventilating Research Association, Laboratory Report. No. 81, 1973.
5 Schwenke, H., "Das Verhalten ebener Horizontaler zuluftstrahlen im begrenzten Raum," Diss. T. U. Dresden, 1973.

6 Hestad, T., Private communication, Institute for VVS, NTH, Trondheim, 1971.
7 Hestad, T., Private communication, Farex Fabrikker, A/S, Norway, 1974.
8 Nielsen, P. V., "Flow in Air Conditioned Rooms," (English translation of PhD thesis from the Technical University of Denmark, 1974), Danfoss A/S, Denmark, 1976.
9 Nielsen, P. V., "Berechnung der Luftbewegung in einem zwangsbelufteten Raum," Gesundheits-Ingenieur, 94, Nr. 10, 1973.
10 Gosman, A. D., Pun, W. M., Runchal, A. K., Spalding, D. B., and Wolfshtein, M., "Heat and Mass Transfer in Recirculating Flows," Academic Press, London, 1969.
11 Pope, S. B., and Whitelaw, J. H., "The Calculation of Near-Wake Flows," *J. Fluid Mech.*, Vol. 73, 1976, p. 9.
12 Gosman, A. D., Khalil, E. E. and Whitelaw, J. H., "The Calculation of Two-Dimensional Turbulent Recirculating Flows," *Proceedings of Symposium on Turbulent Shear Flows*, University Park, Pennsylvania, 1977.
13 Durst, F., Melling, A., and Whitelaw, J. H., *Principles and Practice of Laser-Doppler Anemometry*, Academic Press, London, 1976.
14 Wigley, G., "The Application of Radial Diffraction Gratings to Laser Anemometry," Atomic Energy Research Establishment, report 7886, 1974.
15 Melling, A., and Whitelaw, J. H., "Seeding of Gas Flows for Laser Anemometry," *DISA Information*, Vol. 15, 1973, 5.
16 Schwarz, W. H., and Cosart, W. P., "The Two-Dimensional Turbulent Wall-Jet," *J. Fluid Mech.*, Vol. 10, 1961, p. 481.
17 Gosman, A. D., and Pun, W. M., Lecture notes for the course entitled "Calculation of Recirculating Flows," Imperial College, Heat Transfer Section, Report HTS/74/2, 1974.
18 Nelson, J. L., "An Experimental Investigation of the Turbulent and Mean Flow Properties of a Plane Two-Dimensional Turbulent Wall Jet," Dissertation, University of Tennessee, Dept. of Chem. Eng., 1969.
19 *ASHRAE Handbook of Fundamentals*, New York, 1972.
20 Schwartzbach, G., Private communication, Dept. of Fluid Mech., DTH, Copenhagen, 1973.
21 Förthmann, E., "Über Turbulente Strahlausbreitung," Ing. Archiv, Vol. 5, 1934.
22 Glauert, M. B., "The Wall Jet," *J. Fluid Mech.*, Vol. 1, 1956, p. 625.

APPENDIX 1

Values of Γ_ϕ and S_ϕ in the equation

$$\frac{\partial}{\partial x}(\rho U\phi) + \frac{\partial}{\partial y}(\rho V\phi) = \frac{\partial}{\partial x}\left(\Gamma_\phi \frac{\partial \phi}{\partial x}\right) + \frac{\partial}{\partial y}\left(\Gamma_\phi \frac{\partial \phi}{\partial y}\right) + S_\phi.$$

ϕ	Γ_ϕ	S_ϕ
1	0	0 (Continuity)
U	μ_{eff}	$-\frac{\partial P}{\partial x} + \frac{\partial}{\partial x}\left(\mu_{eff}\frac{\partial U}{\partial x}\right) + \frac{\partial}{\partial y}\left(\mu_{eff}\frac{\partial V}{\partial x}\right)$
V	μ_{eff}	$-\frac{\partial P}{\partial y} + \frac{\partial}{\partial x}\left(\mu_{eff}\frac{\partial U}{\partial y}\right) + \frac{\partial}{\partial y}\left(\mu_{eff}\frac{\partial V}{\partial y}\right)$
κ	μ_{eff}/σ_κ	$G - \rho\epsilon$
ϵ	$\mu_{eff}/\sigma_\epsilon$	$\frac{\epsilon}{k}(C_1 G - C_2 \rho\epsilon)$

$$\mu_{eff} = \mu + \mu_t = \mu + \rho C_\mu K^2/\epsilon$$

$$G = \mu_t\left[2\left\{\left(\frac{\partial U}{\partial x}\right)^2 + \left(\frac{\partial V}{\partial y}\right)^2\right\} + \left(\frac{\partial U}{\partial y} + \frac{\partial V}{\partial x}\right)^2\right]$$

Corresponding constants: $C_\mu = 0.09$; $C_1 = 1.44$; $C_2 = 1.92$; $\sigma_k = 1.0$; $\sigma_\epsilon = 1.22$

APPENDIX 2

Profiles of Longitudinal Velocity in Turbulent Wall Jets

The first known experimental investigation on the plane wall jet was done by Förthmann [21], who was able to reduce all mean velocity data to a single profile, when normalized by the jet thickness and maximum longitudinal velocity. The similarity problem of the radial and plane wall jets was later studied by Glauert [22], and Schwarz and Cosart [16]. The latter deduced the following expressions for the velocity scale U_m (maximum velocity across the jet) and length scale δ_u (thickness of the jet at $U_m/2$ in the outer layer):

$$\frac{U_m}{U_0} = C_u\left(\frac{x - x_D + x_0}{h}\right)^{e_u}$$

$$\delta_u = C_{\delta u}(x - x_D + x_0)$$

where x_D and $-x_0$ are the coordinates of the inlet plane and the virtual origin of the jet - see Fig. 5(*e*).

Current practice in the design of air conditioning systems is to assume that different inlet arrangements originate self-similar turbulent jets which may still be fitted by a suitable set of values of x_0, C_u, e_u and $C_{\delta u}$. Works by Schwartzbach [20] and the *ASHRAE Handbook of Fundamentals* [19] support this assumption for several types of diffuser.

Table 2 summarizes the values for the previous coefficients associated with the experimental data used in section 4.

Table 2

Data	x_0/h	C_u	e_u	$C_{\delta u}$
Schwarz and Cosart	11.2	5.395	−0.555	0.0678
Present measurements	15.2	5.72	−0.555	0.0678
Hestad (1971)	0.0	3.6	−0.5	0.0678
Hestad (1974)	34.0	3.1	−0.5	0.1
Schwartzbach ($y_d/h = 5$)	17.5	3.622	−0.5	0.062
" ($y_d/h = 8.3$)	25.0	3.640	−0.5	0.071
" ($y_d/h = 15$)	49.5	3.462	−0.5	0.070